Proceedings of the Fifth Annual LHCP
CMS-CR-2017/XXX
May 29, 2017

New results on Higgs properties

Jónatan Piedra

On behalf of the ATLAS and CMS Collaborations,
Instituto de Física de Cantabria
(CSIC - Universidad de Cantabria), Spain

ABSTRACT

We present the latest ATLAS and CMS measurements of several Higgs properties, such as signal-strength modifiers for the main production modes, fiducial and differential cross sections, and the Higgs mass. We have analyzed the 13 TeV proton-proton LHC collision data recorded in 2016, corresponding to integrated luminosities up to 36.1 fb^{-1}. Results for the $\text{H} \to \text{ZZ} \to 4\ell$ ($\ell = \text{e}\mu$), $\text{H} \to \gamma\gamma$, and $\text{H} \to \tau\tau$ decay channels are presented. In addition, searches for new phenomena in the $\text{H} \to \gamma\gamma + E_{\text{T}}^{\text{miss}}$ and $\text{H} \to \text{b}\overline{\text{b}} + E_{\text{T}}^{\text{miss}}$ decay channels are presented.

PRESENTED AT

The Fifth Annual Conference
on Large Hadron Collider Physics
Shanghai Jiao Tong University, Shanghai, China
May 15-20, 2017

Patient	Initial level(μg/cc)	w. Magnet	w. Magnet and Sound
Guglielmo B.	0.12	0.10	0.001
Ferrando di N.	0.15	0.11	< 0.0005

Table 1: Place the caption here.

1 Introduction

The discovery of the Higgs boson was announced in 2012 by the ATLAS and CMS collaborations [1, 2] based on proton-proton collisions collected at the CERN LHC at the centre of mass energies of 7 and 8 TeV. Since then a huge effort has been made in the determination of the properties of this newly found particle. The dataset already collected at 13 TeV allows inclusive Higgs boson measurements to be repeated. Furthermore, the increased centre-of-mass energy results in much larger cross sections for events at high partonic centre-of-mass energy. This implies improved sensitivity to a variety of interesting physics processes, such as Higgs bosons produced at high transverse momentum.

In this document we present the latest ATLAS and CMS measurements of several Higgs properties in different decay channels, such as $\mathrm{H} \to \mathrm{ZZ}$, $\mathrm{H} \to \gamma\gamma$ and $\mathrm{H} \to \tau\tau$. In addition, we also present results on searches for phenomena beyond the Standard Model, in Higgs decays to $\gamma\gamma$ or $\mathrm{b\bar{b}}$, with $E_{\mathrm{T}}^{\mathrm{miss}}$ in the final state.

2 $\mathrm{H} \to \mathrm{ZZ}$

The $\mathrm{H} \to \mathrm{ZZ} \to 4\ell$ decay channel ($\ell = \mathrm{e}, \mu$) has a large signal-to-background ratio due to the complete reconstruction of the final state decay products and excellent lepton momentum resolution, making it one of the most important channels for studies of the Higgs boson's properties. Here we present measurements of properties of the Higgs boson in this channel at 13 TeV, for both the ATLAS and CMS collaborations [3, 4].

See Figure 1 and Table 1.

3 $\mathrm{H} \to \gamma\gamma$

See Figure 2.

4 $\mathrm{H} \to \tau\tau$

To establish the mass generation mechanism for fermions, it is necessary to demonstrate the direct coupling of the scalar boson to fermions, and the proportionality of its strength to the fermion mass. The most promising decay channel is $\tau\tau$, because of the large event rate expected in the SM compared to the other leptonic decay modes, and of the smaller contribution from background events with respect to the $\mathrm{b\bar{b}}$ channel. Here we report the results of a search for the SM scalar boson using 35.9 fb^{-1} at 13 TeV, when it decays to a pair of τ leptons [5]. The four τ-pair final states with the largest branching fractions, $\mu\tau_{\mathrm{h}}$, $\mathrm{e}\tau_{\mathrm{h}}$, $\tau_{\mathrm{h}}\tau_{\mathrm{h}}$, and $\mathrm{e}\mu$, are studied.

The search for an excess of SM scalar boson events over the expected background involves a global maximum likelihood fit based on two-dimensional distributions in all channels, together with control regions for the $\mathrm{t\bar{t}}$, QCD multijet and W+jets backgrounds. Figure 3 shows the distribution observed, together with the expected background and signal distributions, in the $\tau_{\mathrm{h}}\tau_{\mathrm{h}}$ channel and VBF category. The signal prediction for a scalar boson with $m_{\mathrm{H}} = 125$ GeV is normalized to its best-fit cross section times branching fraction. The background distributions are adjusted to the results of the global maximum likelihood fit.

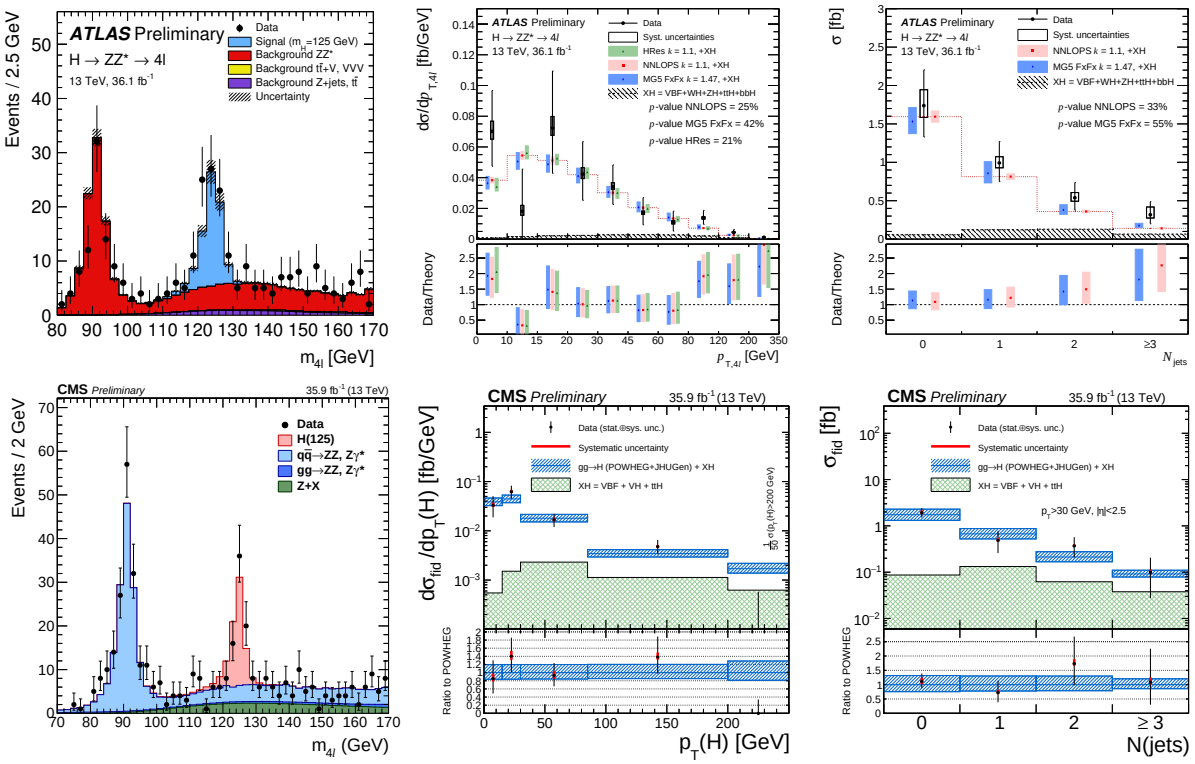

Figure 1: (Top left) ATLAS four-lepton invariant mass distribution of the selected events. The systematic uncertainty on the prediction is shown by the dashed band. (Top center and right) ATLAS differential fiducial cross sections, for the transverse momentum of the Higgs boson (center) and the number of jets (right). The measured cross sections are compared to different ggH predictions, and predictions for all other Higgs production modes XH are added. (Bottom left) CMS four-lepton invariant mass distribution of the selected events. (Bottom center and right) CMS differential fiducial cross sections, for the transverse momentum of the Higgs boson (center) and the number of jets (right). The sub-dominant component of the signal (VBF + VH + ttH) is denoted as XH.

5 Searches for new phenomena

6 Conclusions

References

[1] G. Aad *et al.* [ATLAS Collaboration], Phys. Lett. B **716**, 1 (2012) [arXiv:1207.7214 [hep-ex]].

[2] S. Chatrchyan *et al.* [CMS Collaboration], Phys. Lett. B **716**, 30 (2012) [arXiv:1207.7235 [hep-ex]].

[3] G. Aad *et al.* [ATLAS Collaboration], ATLAS-HIGG-2016-25.

[4] CMS Collaboration [CMS Collaboration], CMS-PAS-HIG-16-041.

[5] CMS Collaboration [CMS Collaboration], CMS-PAS-HIG-16-043.

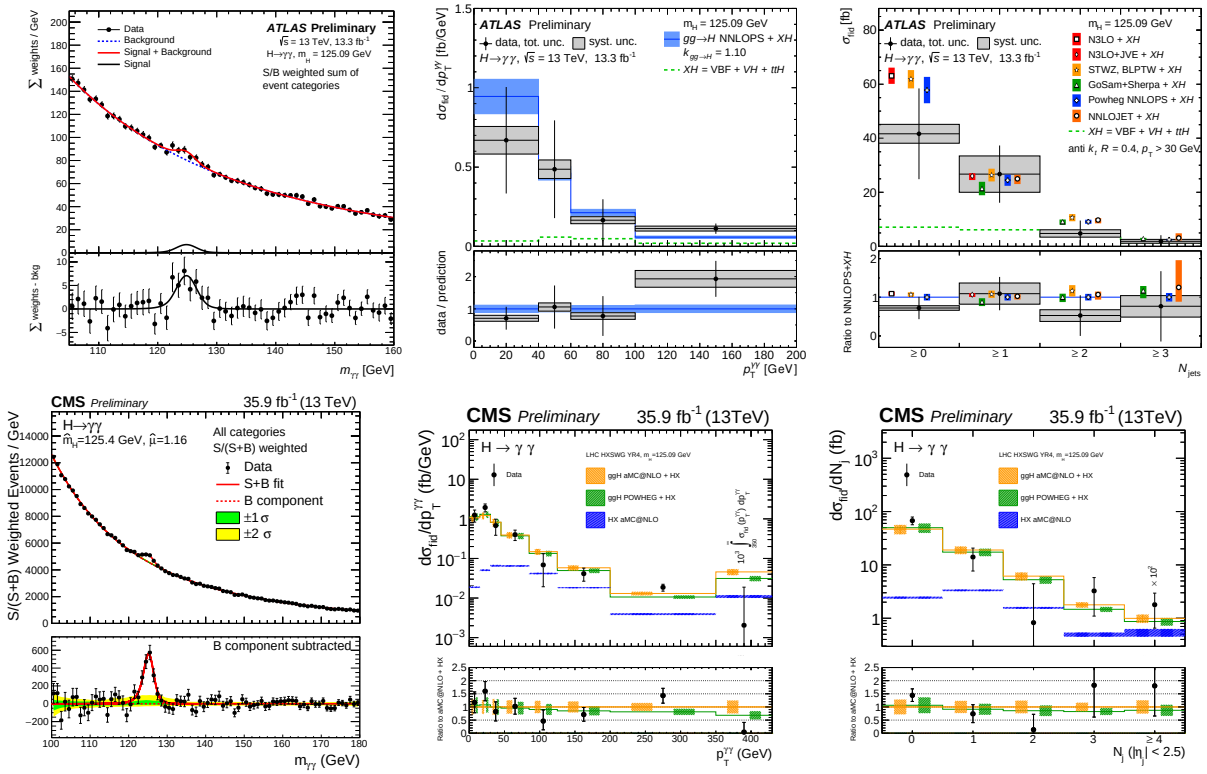

Figure 2: (Top left) ATLAS diphoton invariant mass spectrum. (Top center and right) ATLAS differential fiducial cross sections, for the transverse momentum of the Higgs boson (center) and the number of jets (right). (Bottom left) CMS diphoton invariant mass spectrum. (Bottom center and right) CMS differential fiducial cross sections, for the transverse momentum of the Higgs boson (center) and the number of jets (right).

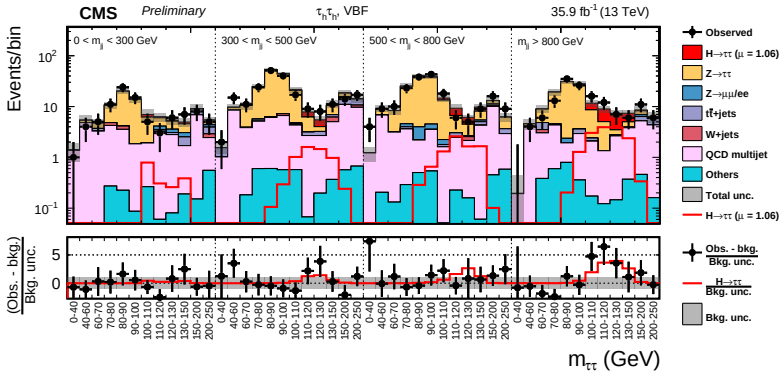

Figure 3: Observed and predicted 2D distributions in the VBF category of the $\tau_h\tau_h$ final state. The normalization of the predicted background distributions corresponds to the result of the global fit. The signal distribution is normalized to its best-fit signal strength.